

# Lysozyme and bovine serum albumin adsorption on uncoated silica and AlOOH-coated silica particles: the influence of positively and negatively charged oxide surface coatings

Kurosch Rezwan<sup>a,b,\*</sup>, Lorenz P. Meier<sup>a,b</sup>, Ludwig J. Gauckler<sup>b,c</sup>

<sup>a</sup>Nonmetallic Inorganic Materials, Department Materials, ETH Zurich, Switzerland

<sup>b</sup>Nichtmetallische Werkstoffe, Wolfgang-Pauli-Str. 10, ETH Hönggerberg, HCI G 538, 8093 Zürich, Switzerland

<sup>c</sup>Nichtmetallische Werkstoffe, Wolfgang-Pauli-Str. 10, ETH Hönggerberg, HCI G 535, 8093 Zürich, Switzerland

Received 6 September 2004; accepted 13 November 2004

## Abstract

The adsorption of lysozyme and bovine serum albumin on silica and AlOOH-coated silica particles—representing negatively and positively charged oxide surfaces—was investigated. The protein-treated uncoated and completely AlOOH-coated silica particles were characterized by zeta potential analysis and UV/VIS spectroscopy. It was found that at pH 7 a protein oppositely charged to the oxide surface adsorbs in significantly higher amounts. In contrast, proteins of the same charge did not or only in very low amounts adsorbed on an oxide surface. As both oxide surfaces were measured to be very hydrophilic it can be concluded that electrostatic interactions dominate the adsorption process at the investigated experimental conditions. The pH regions where the proteins interact via attractive and repulsive coulomb interaction with the particular oxide surfaces were calculated and outlined. © 2004 Elsevier Ltd. All rights reserved.

**Keywords:** Protein adsorption; Surface charge; Silica; Alumina; Sol–gel

## 1. Introduction

Protein adsorption on surfaces of biomaterials and medical implants is an essential aspect of the cascade of biological reactions taking place at the interface between a synthetic material and the biological environment. Type, amount and conformation of adsorbed proteins mediate subsequent adhesion, proliferation and differentiation of cells and are believed to steer foreign body response and inflammatory processes [1–3].

Concerning the protein adsorption process, the fundamental electrostatic interactions between ceramic particles and proteins are only fragmentarily investigated and not well understood [4–10]. Especially, the

influence of particle shape, size and size distribution may vary when studying the adsorption of proteins on different colloids. This can be eliminated by using a sol–gel technique to modify the surface chemistry of narrowly distributed particles. This is possible by coating well-defined silica particle surfaces using a relatively simple and cost-effective method. It is a convenient way to tailor the surface chemistry of a substrate without changing the substrate itself which can particularly be useful for e.g. biosensor applications.

The sol–gel process was used to alter the surface properties of the silica particles in order to investigate the influence of the surface charge on the adsorbed amount of lysozyme (LSZ) and bovine serum albumin (BSA). The coating process was optimized and the coating quality controlled by measuring the zeta potential and by scanning electron microscopy. The precursor used for the coating process was Al-sec-butoxide. The silica particles (negatively charged at pH 7) were coated

\*Corresponding author. Nichtmetallische Werkstoffe, Wolfgang-Pauli-Str. 10, ETH Hönggerberg, HCI G 538, 8093 Zürich, Switzerland. Tel.: +41 1 632 68 53; fax: +41 1 632 11 32.

E-mail address: [kurosch.rezwan@mat.ethz.ch](mailto:kurosch.rezwan@mat.ethz.ch) (K. Rezwan).

with an AIOOH layer which is positively charged at pH 7. We investigated the amounts and the resulting zeta potentials of bovine serum albumin (BSA, negatively charged at pH 7) and lysozyme (LSZ, positively charged at pH 7) adsorbed onto the negatively and positively charged oxide particles to monitor the effect of electrostatic attraction and repulsion on the amount of adsorbed proteins.

## 2. Experimental

### 2.1. Materials and reagents

#### 2.1.1. Silica and Al-sec-butoxide

Silica Snowtex ZL (Lot. No. 140828) was obtained from Nissan Chemicals Industries Ltd. as a 30 vol% suspension. To lower the salt content, the suspension was dialyzed for a few days using a dialysis tube (ZelluTrans ROTH) till the electrical conductivity fell below 1  $\mu\text{S}/\text{cm}$ . The specific surface area was characterized by X-ray disc centrifuge sedigraph and was found to be 34  $\text{m}^2/\text{g}$  with a  $d_{50}$  particle diameter of 0.097  $\mu\text{m}$ .

Al-sec-butoxide was obtained from Fluka (Lot. & Filling: 431389/143502) and was used without further modifications.

Double deionized water with an electrical resistance of 18  $\text{M}\Omega\text{cm}$  from a NANOpure water system (Barnstead) was used for all experiments.

#### 2.1.2. Proteins and protein reagent

Chicken hen egg white lysozyme (LSZ, L6876, Lot. No. 051K7028) and bovine serum albumin (BSA, A7906, Lot. No. 12K1608) were purchased from Sigma Aldrich and used without any modifications. Table 1 shows a comparison of the protein data of LSZ and BSA taken from Ref. [11,12].

Bradford reagent [13] was used as protein dye and was purchased from Sigma Aldrich (B6916, Lot. No. 52K9311) without further modifications.

### 2.2. AIOOH coating of the silica particles

After dialysis, the amount of silica in the suspension was 17 vol% determined by drying the suspension and by pycnometrie. From this suspension a silica suspension of 6 vol% (equal to 8 g silica in 64.4 ml  $\text{H}_2\text{O}$ ) was prepared. Hereafter, the pH was adjusted to 9 by adding drops of a 24%  $\text{NH}_{3\text{aq}}$  solution. The suspension was ultrasonicated with an ultrasound horn for 5 min (UP200s, Dr. Hielscher GmbH, 200 W) at highest performance. The de-agglomerated suspension was poured into a 250 ml two-necked round-bottomed flask and heated up to 85 °C in an oil bath while being stirred. On the flask a reflux water cooler was mounted in order to condensate the evaporating water and to minimize

Table 1  
Protein data of lysozyme (LSZ) and bovine serum albumin (BSA)

Protein	Molecular weight (kDa)	Dimensions ( $\text{nm}^3$ )	Isoelectric point at pH
LSZ [11]	14.3	$3 \times 3 \times 4.5$	11
BSA [12]	66.462	$5 \times 5 \times 5$	4.7–4.9

Table 2  
Different amounts of Al-sec-butoxide added to the silica suspension during the coating process

Added mass Al-sec-butoxide (g)	Al-sec-butoxide/silica (wt/wt%)	Al-sec-butoxide/silica surface area ( $10^{-2} \text{g}/\text{m}^2$ )
9.16	115	3.3
5.725	72	2.06
4.3	54	1.55
2.86	36	1.03

water losses during the coating process. After reaching a constant temperature of 85 °C, the required amount of Al-sec-butoxide was mixed with 70 ml water and poured into the flask. The different amounts used for the coatings are shown in Table 2.

The Al-sec-butoxide reaction with the suspension was kept at 85 °C for 2 h under stirring conditions. Afterwards the suspension was cooled down to below 40 °C. The pH was adjusted to 3 with 2N HCl in order to dissolve residues of amorphous AIOOH. The acidic suspension was stirred for another 10 min and subsequently ultrasonicated for 5 min. The suspension was centrifuged at 2200g for 30 min in a thermostated Hermle Z 513 K. The supernatant was removed and the sediment dispersed in double-deionized water followed by an ultrasound treatment of 5 min. The wt% content was determined by drying 1 ml of the suspension. The particle density was measured by pycnometrie. Based on the vol% of silica found, water was added to dilute the obtained suspension to a 2 vol% suspension for all adsorption and zeta potential measurements. The particle size distribution was measured with an X-ray disc sedigraph (XDC, Brookhaven Instruments) and the surface tension at the air interface by the drop pendant method (PAT 1, SINTERFACE) [14].

All side products during the coating process were removed by the centrifugation step and the protein adsorption was carried out at low ionic strengths ( $<1 \text{ mM KCl}$  as determined by conductometry) and without any organic residues.

### 2.3. Protein addition to the suspension

We added  $4.96 \times 10^{-12}$  mol proteins per  $\text{cm}^2$  silica surface area to the uncoated and coated silica suspension in

order to have the same ratio of protein number to surface area. According to the molecular weights from Table 1, this equals 330 ng/cm<sup>2</sup> BSA, respectively, 71 ng/cm<sup>2</sup> LSZ. The proteins were first dissolved in water and then added. The suspensions were stirred for 16 h in glass bottles with fastened lids at a room temperature of 25 °C.

## 2.4. Measurement methods

### 2.4.1. Zeta potential

After 16 h of stirring the suspensions, 30 ml samples were withdrawn for measurements. The samples were titrated with 1 N HNO<sub>3</sub>, respectively, 1 N KOH and the corresponding zeta potential measured as a function of pH. After each addition of the titrant (base, respectively, acid) an equilibration time of at least 30 s was allowed. The zeta potential of the suspension was measured using the electroacoustic colloidal vibration current (CVI) technique (DT 1200, Dispersion Technology) [15]. This method characterizes the zeta potential by means of a probe that uses ultrasound as a driving force for generating an electroacoustic effect. The probe is a stainless-steel cylinder with a diameter of 3 cm and a length of 10 cm with a piezo-electric transducer inside. This transducer converts an electrical tone-burst into an acoustic pulse that is then emitted into the suspension. The default frequency is 3 MHz. The ultrasonic pulse generates in the suspension a polarization of the colloid particles and their cloud of counterions which can be detected by two electrodes immersed in the suspension. This polarization signal can be used to compute the zeta potential of the particles using electroacoustic theory [15].

The zeta potential measurements were used to control the AIOOH coating quality on silica and to monitor the protein adsorption on the particles.

### 2.4.2. Determination of the adsorbed protein amount by UV/VIS spectroscopy

To study the protein adsorption amount, proteins were dissolved in water and then added to the powder suspensions. The suspensions were equilibrated for 16 h at room temperature under stirring conditions. The pH was adjusted to 7.

To determine the amount of surface adsorbed protein four samples of 1.5 ml were withdrawn from each suspension at pH 7 after 16 h and filled into plastic centrifuge cuvettes. Subsequently, the cuvettes were centrifuged for 10 min at 3800g in an Eppendorf 5417R table centrifuge which was thermostated at 25 °C. The supernatants were transferred to fresh cuvettes and centrifuged again. The protein concentrations of these supernatants were measured by using the Bradford method [13]. According to the Bradford method the VIS absorption values of the protein

concentration samples were measured at the wavelength of 595 nm, using an UV/VIS spectrometer (Lambda 2, Perkin Elmer). The results were compared to reference curves for the specific protein with a detection limit of 0.007 mg/ml. From the protein concentration left in the supernatant and the total amount of protein added in the beginning, the protein amount adsorbed was calculated.

## 3. Results

### 3.1. AIOOH coating of silica particles

In Fig. 1 the zeta potential of uncoated silica (0 wt/wt%) and coated silica with different amounts of Al-sec-butoxide additions relative to the silica weight (36, 54, 72 and 115 wt/wt%) are plotted versus pH. The surface charge of the uncoated silica particles is negative for the entire pH range measured with an IEP found at pH 1.1. The IEPs of the coated samples differ significantly from that of the uncoated silica particles. The IEP shifts from pH 1.1 to a maximum pH of 8.7 after an addition of 115 wt/wt% Al-sec-butoxide (Fig. 2). These data verify that at this added amount the surface chemistry of the silica particles is determined by that of AIOOH only.

The mean diameter obtained by the X-ray sedigraph of the uncoated silica particles was found to be at 97 nm, respectively, at 102 nm for the coated particles (Fig. 3). The resulting coating thickness was 2.5 nm. The surface tensions measured at pH 7 for 2 vol% suspensions and water as a reference are listed in Table 3. No significant change in surface tension could be observed.

Dried samples of uncoated silica particles and with 115 wt/wt% Al-sec-butoxide were investigated by SEM

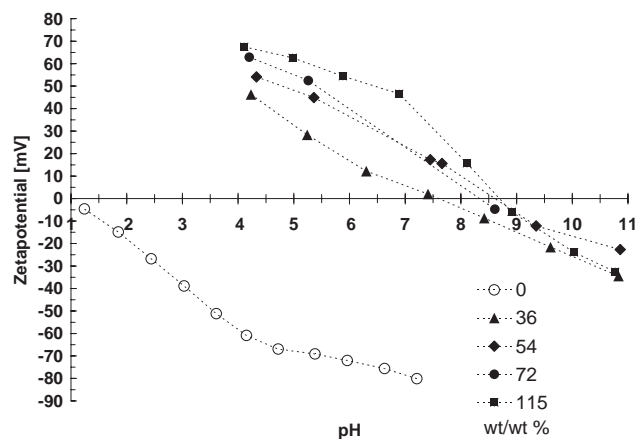


Fig. 1. Zeta potential of silica particles with different wt/wt% additions of Al-sec-butoxide relative to the silica weight present in suspension.

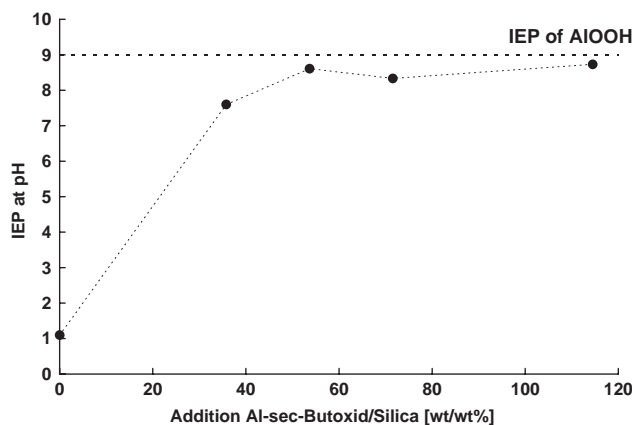


Fig. 2. Shift of IEP as a function of Al-sec-butoxide addition in wt/wt% derived from Fig. 1. The dotted horizontal line indicates the IEP of AlOOH known from Ref. [16].

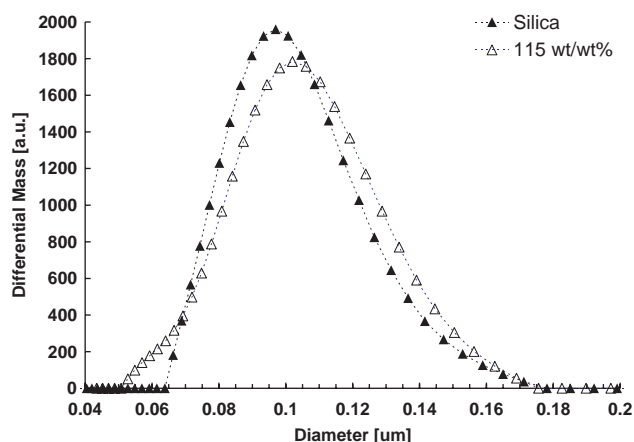


Fig. 3. Particle size distribution of uncoated and coated (115 wt/wt%) silica. The main diameter for the uncoated silica particles was found at 0.097 μm, respectively, at 0.102 μm for the coated particles. The resulting coating thickness is 2.5 nm.

Table 3  
Surface tensions of 2 vol% suspensions measured by the drop pendant method at pH 7

	Water	Silica 2 vol%	AlOOH-coated silica 2 vol%
Surface tension (mN/m)	72.8 ± 0.2	72.5 ± 0.4	71.5 ± 0.2

as shown in Figs. 4 and 5. In both cases the particles are not attached to each other. At a higher magnification the coated silica particles revealed a slightly rougher surface than the uncoated particles. In contrast, Fig. 6 shows the rather rough surfaces of coated silica particles after a not yet optimized coating procedure with an excess of Al-sec-butoxide (575 wt%/wt%) during the reaction. The silica particles were bound to each other

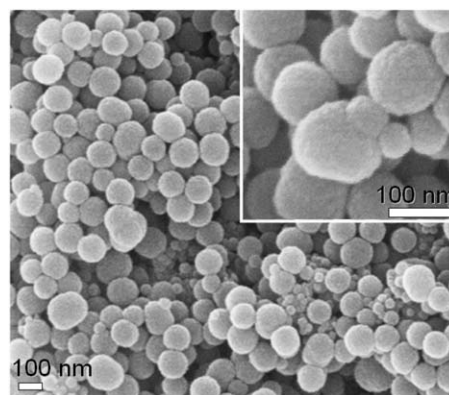


Fig. 4. SEM micrographs of the uncoated spherical silica particles.

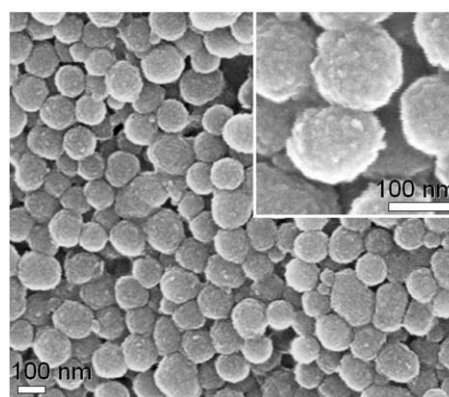


Fig. 5. SEM micrographs of AlOOH-coated silica particles (115 wt/wt%) obtained by the optimized sol-gel process. The close up picture reveals the surface being coated and less smooth than in Fig. 4.

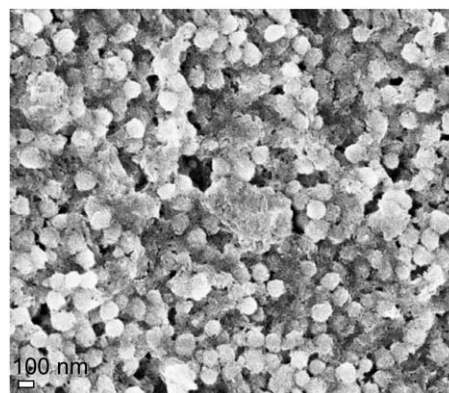


Fig. 6. This SEM micrograph shows a preliminary result with no process optimization for a 575 wt/wt% Al-sec-butoxide/silica ratio. The excess of Al-sec-butoxide during the coating process precipitated between the silica particles and agglomerates were obtained.

and undesired agglomerates were obtained. Such lots with agglomerates were not used for zeta potential and protein adsorption measurements due to the expected irreproducibility of the results.

### 3.2. Protein adsorption

For all protein adsorption measurements the coating process with the IEP closest to pH 9 was used, that is an addition of Al-sec-butoxide of 115 wt%/wt% relative to the silica weight present in the suspension according to Fig. 2. At this amount the oxide surface chemistry is clearly determined by AlOOH.

Fig. 7 shows the zeta potential curves for uncoated silica with additions of LSZ and BSA as a function of pH. After protein adsorption the IEP of the silica particles shifts from the native pH 1.1 to 4.6 in the case of BSA, and to pH 10.3 for LSZ.

In Fig. 8, the zeta potential curves of the coated silica particles with additions of LSZ and BSA are plotted as a function of pH. The adsorption of BSA shifts the IEP of the suspension from pH 8.7 down to pH 7. In contrast to this, the adsorption of LSZ shifts

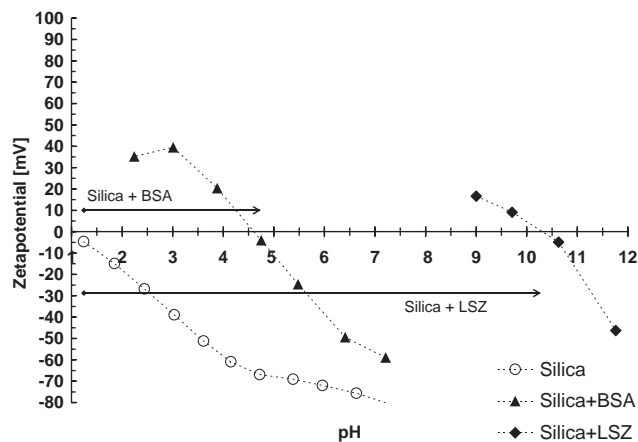


Fig. 7. Zeta potential of uncoated silica with addition of BSA and LSZ after 16 h of adsorption time. The arrows indicate the shift of IEP after protein addition.

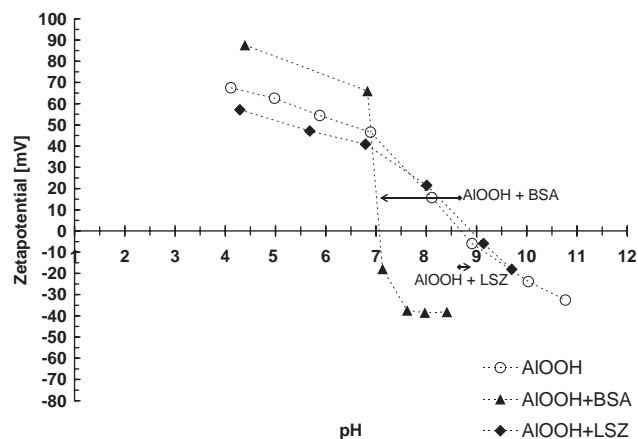


Fig. 8. Zeta potential of coated silica (= AlOOH) with additions of BSA and LSZ after 16 h of adsorption time. The arrows indicate the shift of IEP after protein addition.

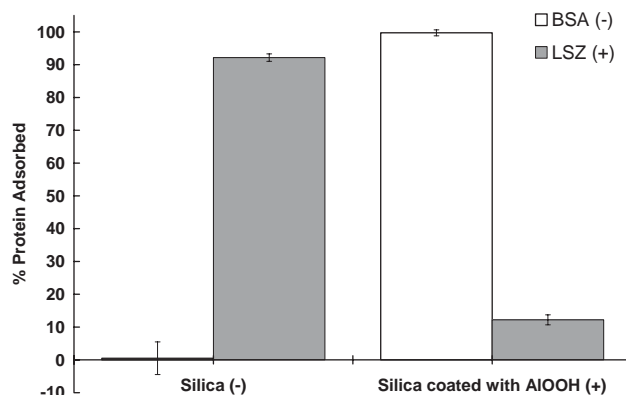


Fig. 9. Percentage of initial protein amount adsorbed at pH 7 after 16 h detected by UV/VIS spectroscopy. The signs in the brackets indicate if the particle surfaces, respectively, the proteins carry positive or negative net charges at pH 7.

the IEP closer to pH 9 as expected from the LSZ IEP which is at pH 11 [11].

The percentage of initial amount of BSA, respectively, LSZ ( $4.96 \times 10^{-12} \text{ mol/cm}^2$ ), adsorbed on the different oxide surfaces are plotted in Fig. 9. The UV/VIS spectroscopy measurements were carried out at pH 7 after 16 h of equilibration time. The adsorption amount of LSZ onto silica is almost 100% while only 10% adsorbed onto AlOOH-coated silica particles. On the other hand, about 100% of the initial BSA amount adsorbed onto AlOOH-coated silica while almost no BSA adsorbed on untreated silica.

## 4. Discussion

### 4.1. AlOOH coating quality of silica particles

According to Figs. 1 and 2 the addition of Al-sec-butoxide of 115 wt/wt% ( $3.3 \times 10^{-2} \text{ g/m}^2$ ) produced coatings which resulted in an IEP of pH 8.7. This value is in good agreement with the IEP for AlOOH found in Ref. [16]. The SEM analysis of the uncoated (Fig. 4) and coated (Fig. 5) silica particles clearly show a change of surface smoothness and verify that the silica particles have a coating of AlOOH. Using higher amounts of Al-sec-butoxide did not result in a further shift of the IEP. On contrary, higher amounts of Al-sec-butoxide resulted in undesired AlOOH precipitates which led to agglomeration of the particles as shown by the SEM micrograph (Fig. 6). Agglomerate-free coatings could be obtained for Al-sec-butoxide additions of 115 wt%/wt% or less, as confirmed by the particle size distribution analysis shown in Fig. 3.

The surface tension of the silica particles does not change after coating as shown in Table 3. The surface tension is very close to water for uncoated and coated silica. The surface remains hydrophilic.

#### 4.2. Correlation of protein adsorption and zeta potential

LSZ adsorption onto coated and uncoated silica shifts the IEP of the suspension closer to pH 11, corresponding to the IEP of the protein [11]. On the other hand, BSA adsorption shifts the IEP towards the IEP of BSA [12] which is at a pH of around 5 (Figs. 7 and 8).

From the protein adsorption amount shown in Fig. 9 it can be concluded that the amount of adsorbed protein strongly corresponds to the sign of the net charge of the protein and of the particle surface. BSA, which is negatively charged at a pH of 7, adsorbs nearly 100% on the positively charged surface of AlOOH. The opposite observation was made for LSZ which is positively charged at the pH of 7. LSZ adsorbs almost completely on the negatively charged silica surface but hardly adsorbs onto the positively charged AlOOH. From these observations it can be concluded that electrostatic interaction governs the adsorption process at pH 7 for the two investigated proteins and oxide surfaces. The hydrophobic effect does not play an important role as the silica and the AlOOH-coated surfaces are both very hydrophilic (see Table 3).

Interestingly, the very low amount of adsorbed BSA on silica (adsorption maximum of 8% as indicated by the error bar) shifts the IEP of silica from pH 1.1 to a pH of about 4.5 as shown in Fig. 7. The reason for this substantial shift of IEP is not clear. In order to find out which amino acids govern protein adsorption at which pH, a protein specific amino acid charge distribution can be calculated. Taking into account the pK values of the 7 amino acid side chains which are able to carry charges the dissociation ratio for each amino acid can be calculated and multiplied by the number of the specific amino acid present in the particular protein. More details about the calculation method and the pK values of the amino acids can be found elsewhere [17,18].

The amino acid charge distributions versus pH for BSA and LSZ are plotted in Figs. 10 and 11, respectively. At pH 7, only Arginin, Lysin are positively charged and Asparaginacid, Glutaminacid negatively charged. The other amino acids do not carry any charges at pH 7. The greyly shaded regions in the plots indicate qualitatively the net surface charges of the oxide surfaces based on the zeta potential measurements from Figs. 7 and 8. The functional groups from which the different amino acid charge states originate are mainly due to carboxyl ( $-\text{COOH}$ ) and amino groups ( $-\text{NH}_2$ ).

In the basic pH region where a  $-\text{COOH}$  group is deprotonated and oppositely charged to the oxide surface, a formation of a chemical bond is possible by a ligand-exchange reaction. This model was found to govern bonds of small aromatic and aliphatic molecules with carboxyl- and hydroxyl-groups on oxide surfaces in aqueous environment at different pHs in earlier studies [19,20].

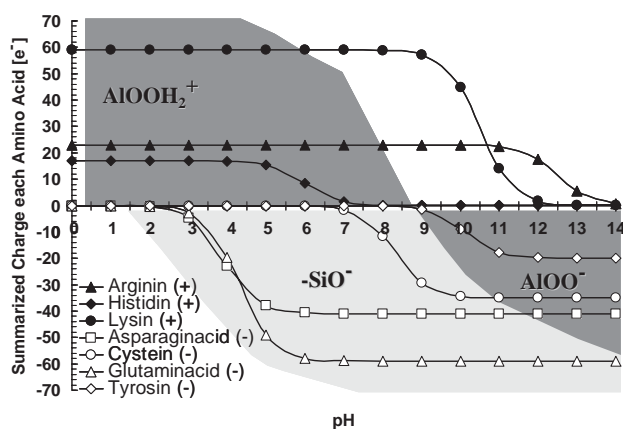


Fig. 10. Amino acid charge distribution calculated as a function of pH for BSA including qualitatively the regions of net surface charges for silica (light grey) and AlOOH (dark grey) derived from the zeta potential measurements of Figs. 7 and 8.

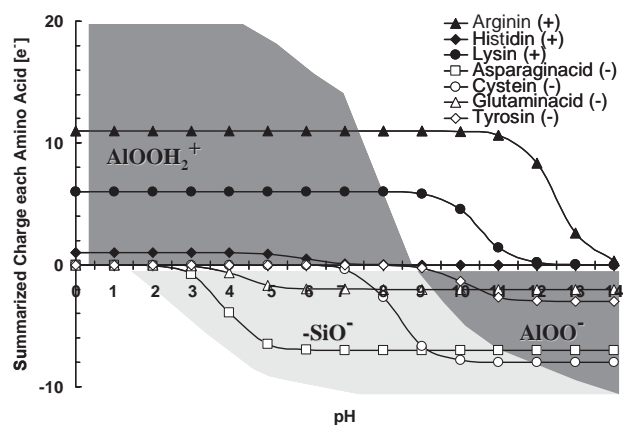


Fig. 11. Amino acid charge distribution calculated as a function of pH for LSZ including qualitatively the regions of net surface charges for silica (light grey) and AlOOH (dark grey) derived from the zeta potential measurements of Figs. 7 and 8.

In the acidic region the  $-\text{NH}_2$  group is protonated ( $-\text{NH}_3^+$ ) and carries a positive charge. It can interact with the negatively charged hydroxyl surface of the oxide particles. These two models are illustrated in Fig. 12.

## 5. Conclusion

Silica particles were coated by a sol-gel technique and the coating quality optimized.

From the amount of LSZ and BSA adsorbed to silica and AlOOH-coated silica particles it was found that positively charged LSZ adsorbs in significantly higher amounts on negatively charged silica particles ( $-\text{SiO}^-$ ) at pH 7 than on positively charged AlOOH<sub>2</sub><sup>+</sup> particles. On the other hand it was found that negatively charged

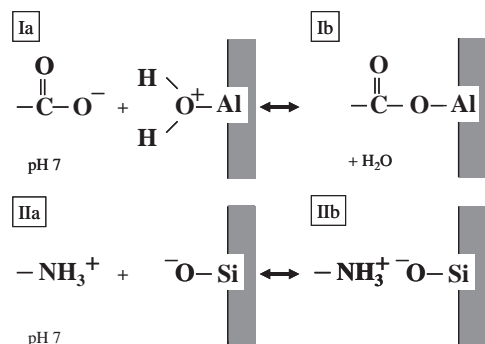


Fig. 12. Ia and Ib illustrate the state before and after the ligand-exchange reaction of a carboxyl group with an alumina hydroxyl group at pH 7. During the reaction one  $\text{H}_2\text{O}$  molecule condensates and a bond is formed. Iia and Iib illustrate the interaction of an amino group with the silica hydroxyl group at pH 7.

BSA adsorbs in significantly higher amounts to positively charged  $\text{AlOOH}_2^+$ -coated particles compared to positively charged LSZ. The prime importance of electrostatic interaction for the proteins LSZ and BSA with  $-\text{SiO}^-$  and  $\text{AlOOH}_2^+$  particle surfaces at pH 7 was demonstrated. Other effects seem to play a minor role under the applied experimental conditions and for hydrophilic oxide surfaces used. The amino acid charge distributions were calculated and superposed with the measured net surface charges of the oxide particles as a function of pH. The pH regions were outlined where proteins with their charged amino acid side chains may experience repulsive and attractive coulomb interactions.

## Acknowledgments

We thank Dr. Walter Caseri for valuable discussions and ETH Zurich for funding this project (TH Fund No. 0-20-148-03).

## References

- [1] Brunette DM, Tengvall P, Textor M, Thomson P. Titanium in medicine—material science, surface science, engineering, biological responses and medical applications. Berlin: Springer; 2001.
- [2] M. Bucciattini EG, Chiti Fabrizio, Baroni F, Formigli L, Zurdo J, Taddei N, Ramponi G, Dobson CM, Stefani M. Inherent toxicity of aggregates implies a common mechanism for protein misfolding diseases. *Nature* 2002;416:507–11.
- [3] Bonfield W. TKE. Biomaterials—a new generation. *Mater World* 1997;5(1):18–20.
- [4] Yuan Y, Oberholzer MR, Lenhoff AM. Size does matter: electrostatically determined surface coverage trends in protein and colloid adsorption. *Colloid Surf A: Physicochem Eng Aspects* 2000;165(1–3):125–41.
- [5] Lee W-K, Ko J-S, Kim H-M. Effect of electrostatic interaction on the adsorption of globular proteins on octacalcium phosphate crystal film. *J Colloid Interface Sci* 2002; 246(1):70–7.
- [6] Kondo A, Oku S, Higashitani K. Structural changes in protein molecules adsorbed on ultrafine silica particles. *J Colloid Interface Sci* 1991;143(1):214–21.
- [7] Kondo A, Higashitani K. Adsorption of model proteins with wide variation in molecular properties on colloidal particles. *J Colloid Interface Sci* 1992;150(2):344–51.
- [8] Kondo A, Mihara J. Comparison of adsorption and conformation of hemoglobin and myoglobin on various inorganic ultrafine particles. *J Colloid Interface Sci* 1996;177(1):214–21.
- [9] Carla E, Giacomelli WN. The adsorption–desorption cycle. Reversibility of the BSA–silica system. *J Colloid Interface Sci* 2001;233(2):234–40.
- [10] Bos MA, Shervani Z, Anusiem ACI, Giesbers M, Norde W, Kleijn JM. Influence of the electric potential of the interface on the adsorption of proteins. *Colloid Surf B: Biointerfaces* 1994;3(1–2):91–100.
- [11] Burton WG, Nugent KD, Slattery TK, Summers BR, Snyder LR. Separation of proteins by reversed-phase high-performance liquid chromatography. I. Optimizing the column. *J Chromatogr A* 1988;443:363–79.
- [12] Carter DC, Ho JX. Structure of serum albumin. *Adv Protein Chem* 1994;45:153–203.
- [13] Bradford MM. A rapid and sensitive method for the quantization of microgram quantities of protein utilizing the principle of protein-dye binding. *Anal Biochem* 1976;72(1/2): 248–54.
- [14] Loglio G, Pandolfini P, Miller R, Makievski AV, Ravera F, Ferrari M, et al. Drop and bubble shape analysis as tool for dilational rheology studies of interfacial layers. In: Möbius RM, editor. Novel methods to study interfacial layers. Amsterdam: Elsevier; 2001. p. 439–84.
- [15] Dukhin AS, Goetz PJ. Ultrasound for characterizing colloids. Particle sizing, zeta potential, rheology. Amsterdam: Elsevier; 2002.
- [16] Parks GA. The isoelectric points of solid oxides, solid hydroxides, and aqueous hydroxo complex systems. *Chem Rev* 1965;65:177–98.
- [17] K. Rezwan LPM, Vörös J, Textor M, Gauckler LJ. Bovine serum albumin adsorption onto colloidal  $\text{Al}_2\text{O}_3$  particles: a new model based on zeta potential- and UV/VIS measurements. *Langmuir* 2004;20(23):10055–61.
- [18] Stryer L. Biochemistry, 5th ed. New York: Freeman & Co.; 2002.
- [19] Kummert R, Stumm W. The surface complexation of organic acids on hydrous Gamma- $\text{Al}_2\text{O}_3$ . *J Colloid Interface Sci* 1980;75(2):373–85.
- [20] Hidber PC, Graule TJ, Gauckler LJ. Influence of the dispersant structure on properties of electrostatically stabilized aqueous alumina suspensions. *J Eur Ceram Soc* 1997;17(2–3):239–49.